

Experimental bounds on masses and fluxes of nontopological solitons

J. Arafune and T. Yoshida

Institute for Cosmic Ray Research, University of Tokyo, Kashiwanoha 5-1-5, Kashiwa 277-8582, Japan

S. Nakamura

Faculty of Engineering, Yokohama National University, Tokiwadai 79-5, Hodogaya-Ku, Yokohama 240-8501, Japan

K. Ogure

Department of Physics, Kobe University, Rokkoudaicho 1-1, Nada-Ku, Kobe 667-8501, Japan

(Received 2 May 2000; published 19 October 2000)

We reanalyze results of various experiments, the original purpose of which was not for the Q -ball or the Fermi-ball searches. Based on these analysis in addition to the available data on Q balls we obtain rather stringent bounds on flux, mass, and a typical energy scale of Q balls and also those of Fermi balls. In case these nontopological solitons are the main component of the dark matter of the galaxy we find that only such solitons with very large quantum numbers are allowed. We also estimate how sensitive the future experiments are to searches for Q balls and Fermi balls.

PACS number(s): 11.27.+d, 95.35.+d, 98.80.Cq

I. INTRODUCTION

In quantum field theory there exist “nontopological solitons,” such as Q balls [1,2], Fermi balls [3,4], and neutrino balls [5], the stabilities of which are based on conservation of global U(1) charges, not on that of topological quantum numbers. For example, Q balls are stabilized by conservation of a U(1) charge [1,2] of scalar fields, while Fermi balls and neutrino balls are stabilized by conservation of the number of such fermions that have Yukawa couplings with scalar fields [3–5]. If such nontopological solitons exist, they may solve or at least be closely related to important problems in cosmology: dark matter [3,4], the baryon number asymmetry of the universe [2,6–8], and γ -ray bursts [5,9].

Although the idea of such nontopological solitons is very attractive, the qualitative properties of them, such as the mass scale, charge size, typical energy scale, and cosmic abundance, are so ambiguous that there are many orders of magnitude in the parameter space to be considered. It is then desirable to make the parameter regions of nontopological solitons as narrow as possible by observational data available now and to make clear what regions are to be searched with experiments in the near future. Although a few useful observational or phenomenological analyses to examine the allowed parameter regions of Q balls have been reported, no comprehensive analyses are available at present. In fact, Kusenko *et al.* [10] discussed the experimental signatures of Q balls and pointed out powerful detection methods for neutral Q balls. The Gyrlyanda experiments at Lake Baikal [11] reported the flux limit of neutral Q balls applying these methods to their monopole search experiments. The report also gave rough estimates of bounds to be obtained with other monopole search experiments, “Baksan” scintillators [12] and old aged mica [13]. Bakari *et al.* [14] calculated the energy losses of Q balls in matter and concluded the various

MACRO detectors can search for charged Q balls.¹ When it comes to Fermi-balls, no experimental limits on the flux have been reported to date.

In the present paper, we make comprehensive discussion on the flux limits of Q balls and Fermi balls. Since their mass could be very large, we use various kinds of results of direct searches for supermassive magnetic monopoles [15], nucleonites, and/or heavy primary cosmic rays [16]. We also estimate sensitivity of present and future experiments (mainly designed for different purposes) about nontopological soliton search stressing the importance of the specific analysis for them. In the following discussion, we analyze the flux bounds taking the charge Z_Q for the case of $Z_Q=0, 1, 2, 3, 10,$ and 137 , as typical values. If the charge is larger than 137 , the Q ball will have the electromagnetic properties at low energy similar to the case of $Z_Q=137$, having a geometrical cross section πR_Q^2 with the effective radius $R_Q \sim 1 \text{ \AA}$ at least [19]. For the case of Fermi-balls, we assume that the electric charge to be large enough to assure its stability against deformation and fragmentation [4], and that the electromagnetic properties at low energy is the same as the case of $Z_F=137$ unless the radius exceeds 1 \AA .

II. EXPERIMENTAL BOUNDS ON Q BALL

A. Q ball properties

In the following our arguments will be restricted to the case of thick wall Q balls, since the most attractive Q balls in supersymmetry (SUSY) are of this case [2]. We briefly review here the properties of Q balls to clarify our notations and assumptions in estimating the flux bounds.

Q balls consist of a complex scalar field with a conserved global U(1) charge. The scalar field, φ vanishes outside the

¹The explicit values of the flux upper limits on Q balls are not available yet.

Q ball, while it forms a coherent state inside with time-dependent phase [1],

$$\varphi(t, \vec{x}) = \varphi(\vec{x}) e^{-i\omega t}. \quad (1)$$

The Q ball is the lowest energy state with a fixed global U(1) charge, and is given by minimizing the Q ball mass M_Q ,

$$M_Q = \int dx [|\partial_t \varphi|^2 + |\vec{\nabla} \varphi|^2 + V(|\varphi|^2)], \quad (2)$$

under the constraint on the charge Q ,

$$Q = i \int dx [\varphi^* \partial_t \varphi - \varphi \partial_t \varphi^*]. \quad (3)$$

Here we assume² that for large φ the scalar potential $V(|\varphi|^2)$ is almost ‘‘flat,’’ i.e., $V(|\varphi|^2) \simeq M_S^4$, where M_S is a constant with a mass dimension. (The potential of this type is known to be present in supersymmetric theories, in which M_S is a SUSY breaking scale.) In this case [10], the Q ball mass is obtained as

$$M_Q = \frac{4\pi\sqrt{2}}{3} M_S Q^{3/4}, \quad (4)$$

with its radius

$$R_Q = \frac{1}{\sqrt{2}} M_S^{-1} Q^{1/4}. \quad (5)$$

The proportionality, $M_Q \propto Q^{3/4}$, in Eq. (4) leads to the stability of the Q ball for Q large enough. If we consider a baryonic Q ball, i.e., a B ball,³ for example, the condition of stability against nucleon emission is $m_{\text{proton}} > (\partial/\partial Q)M_Q$, i.e.,

$$Q > 5.0 \times 10^{14} \left(\frac{M_S}{\text{TeV}} \right)^4. \quad (6)$$

It is pointed out that such large Q balls could be formed in the early universe [8,6,17]. If it happened and such large

²We stress that our result do not lose generality by this assumption. The experimental flux limits, which we obtain later as a function of mass of Q -balls, are independent of the assumption in cases of charged Q -balls, since they depend only on their mass. On the other hand, they are dependent of the assumption in case of neutral Q -balls, since they depend only on their cross section rather than their mass. Of course, the flux limits of the neutral Q -balls were indecent of the assumption if we expressed them as a function of the cross section. Readers, who are interested in neutral Q -balls with another type of potential, can easily accommodate our results by matching the mass of the Q -balls with such of ours, that has the same cross section as them.

³A B ball is the Q ball the conserved U(1) charge of which is baryon number.

stable Q balls have survived till present, they would contribute to the dark matter in the Galaxy. Their flux should then satisfy

$$F \leq F_{\text{DM}} \sim \frac{\rho_{\text{DM}} v}{4\pi M_Q} \sim 7.2 \times 10^5 \left(\frac{\text{GeV}}{M_Q} \right) \text{cm}^{-2} \text{sec}^{-1} \text{sr}^{-1}, \quad (7)$$

where ρ_{DM} is the energy density of the dark matter in our Galaxy, $\rho_{\text{DM}} \sim 0.3 \text{ GeV/cm}^3$, and v is the virial velocity of the Q ball, $v \sim 3 \times 10^7 \text{ cm/sec}$. In the following analysis for Q balls and Fermi balls, we assume for simplicity the velocity of Q balls to be $v = 10^{-3}c$, where c is the light velocity.

In order to estimate efficiencies to detect Q balls with various detectors, Kusenko *et al.* [10] classified relic solitons into two groups according to the properties of their interaction with matter: supersymmetric electrically neutral solitons (SENS) and supersymmetric electrically charged solitons (SECS). In the present paper we use the terms SENS and SECS only for Q balls. In the case of SENS, a process similar to proton decay may occur in the thin layer on the Q ball’s surface, when they collide with nuclei. The energy release of roughly 1 GeV per nucleon is carried away by pions through this process, which we call the ‘‘KKST process’’ after the authors of Ref. [10]. In case of SECS with positive charge, however, the KKST process in collision with nuclei will be strongly suppressed by Coulomb repulsion, and only electromagnetic processes will take place. A charged Q ball with small velocity is accompanied by an atomiclike cloud of electrons, and interacts with matter just like an atom with a heavy mass. If the charge is very large, the effective interaction radius is about 1 Å, which is similar to the case of ‘‘nuclearites’’ [18,19]. Negatively charged Q balls are practically not of much interest to us at present. (If negatively charged Q balls happened to exist, the detection of them should be much easier than that of positively charged ones, since they cause both of electromagnetic process and the KKST process in collision. Thus, the excluded parameter region of the positively charged Q balls is also excluded for the negatively charged ones.) We then discuss only neutral and positively charged Q balls in the following.

B. Bounds on flux and mass of neutral Q balls (SENS)

As pointed out by Kusenko *et al.* [10], a neutral Q ball would produce the KKST process, when it collides with a nucleus, absorbing it and emitting pions with total energy about 1 GeV per nucleon. If the cross section of such process is large and then successive events of this type are detected along a single trajectory, it will be a signal for the Q ball. (We note that such a Q ball processes are different from the Rubakov effect [20] though they are similar to each other. The cross section for the former process does not depend much on whether the target nucleus possesses a magnetic moment or not, while the cross section for the latter process

strongly depends on it.⁴) Since the interaction cross section of the KKST process is expected roughly of a geometrical size, the energy loss of SENS is determined by

$$\frac{dE}{dx} = -\pi R_Q^2 v^2 \rho, \quad (8)$$

similar to the case of nuclearite collision with a nucleus [18,19]. Here R_Q and ρ are the radius of the Q ball and the density of the target matter, respectively. In order that Q balls can reach the detector site and penetrate the detector, the following condition should be satisfied:

$$M_Q \geq \frac{1}{7.3} \pi R_Q^2 \int \rho dx \quad (9)$$

with integration over the trajectory of Q balls. This leads to

$$M_Q \geq 4.2 \times 10^{-39} \left(\frac{\rho L}{\text{gr cm}^{-2}} \right)^3 \left(\frac{\text{TeV}}{M_S} \right)^8 \text{ GeV}, \quad (10)$$

where L is the path length for the Q ball to traverse matter (air, water, and/or rock), and to penetrate the detector. Since we are interested in the parameter regions of $M_S > 100$ GeV, $\rho \leq 10$ gr cm⁻³, $L \leq 2R_{\text{Earth}} \sim 1.3 \times 10^{10}$ gr cm⁻², and $M_Q \gg M_S$, this condition is trivially satisfied in any experiments on the earth.

Most experimental searches for monopole-catalyzed proton decay (the Rubakov effect [20]) are also sensitive to the KKST process, and are able to give useful bounds on SENS flux. Here let us review the available data, not only the already reported results of the Gyrlyanda experiments at Lake Baikal on SENS flux [11] but also other typical experiments reinterpreting them to get SENS flux bounds.

The Gyrlyanda experiments reported that the flux of SENS has the bound [11]

$$F < 3.9 \times 10^{-16} \text{ cm}^{-2} \text{ sec}^{-1} \text{ sr}^{-1},$$

if the cross section for the KKST process is $\sigma > 1.9 \times 10^{-22}$ cm². This corresponds to the lower limit of the SENS mass

$$M_Q > 1.0 \times 10^{21} \left(\frac{M_S}{\text{TeV}} \right)^4 \text{ GeV},$$

since Eq. (4) and Eq. (5) relate σ to M_Q as

$$\sigma = 1.9 \times 10^{-36} \left(\frac{\text{TeV}}{M_S} \right)^{8/3} \left(\frac{M_Q}{\text{GeV}} \right)^{2/3} \text{ cm}^2. \quad (11)$$

The authors of Ref. [11] also estimated the SENS flux limit which will be given by BAKSAN experiments [12]:

⁴If the nucleus has a finite magnetic moment, the cross section of the Rubakov process should have an enhancement factor [21] of $\sim 1/\beta^2 \sim 10^6$ with β being the relative velocity (in unit of the light velocity) between the monopole and the nucleus.

$$F < 3.0 \times 10^{-16} \text{ cm}^{-2} \text{ sec}^{-1} \text{ sr}^{-1},$$

if the cross section is $\sigma > 5.0 \times 10^{-26}$ cm², which corresponds to

$$M_Q > 4.2 \times 10^{15} \left(\frac{M_S}{\text{TeV}} \right)^4 \text{ GeV}.$$

Although the above two experiments give considerably stringent bounds to SENS, let us examine how stringent limits will be given by other monopole searches and future cosmic ray experiments.

The Kamiokande Cherenkov detector [22], which has 3000 tons of water and about 1000 phototubes and is located at about 1000 m deep underground, gave the limits of monopole with 335 days of live time. We roughly reinterpret them as SENS flux limits [34]

$$F < 3 \times 10^{-12}, \quad 3 \times 10^{-14}, \quad \text{and} \\ 3 \times 10^{-15} \text{ cm}^{-2} \text{ sec}^{-1} \text{ sr}^{-1},$$

for SENS with $\sigma = 0.1, 1,$ and 10 mb, which correspond to

$$M_Q = 4.0 \times 10^{11}, \quad 1.2 \times 10^{13}, \quad \text{and}$$

$$3.9 \times 10^{14} \text{ in units of } \left(\frac{M_S}{\text{TeV}} \right)^4 \text{ GeV},$$

respectively. Note that in case of $\sigma > 100$ mb which corresponds to $M_Q > 1.2 \times 10^{16}$ GeV, the detection efficiency would get less due to the difficulty to identify successive events as discrete ones. Taking this into account, we conservatively exclude the region, $4.0 \times 10^{11} \text{ GeV} \leq M_Q \leq 1.2 \times 10^{16} \text{ GeV}$, by the Kamiokande experiments. The super-Kamiokande experiments with a 50 000 ton water Cherenkov detector would obtain more stringent flux limits than those of Kamiokande by about two orders of magnitude with three years of observation time.

The MACRO, large underground detectors [14,23,24] consisting of three kinds of subdetectors, i.e., scintillation counters, streamer tubes and nuclear track detectors (CR-39) could search for SENS [14]. In Ref. [14], the flux limits of SENS are reported to be obtained as $F \leq 10^{-16} \text{ cm}^{-2} \text{ sec}^{-1} \text{ sr}^{-1}$. The detection efficiency is, however, difficult for us to estimate the flux limit to be obtained is not given here.

The AMANDA Cherenkov detectors [25,26] at the South Pole under ice are designed mainly to detect relativistic particles. If they could also detect slow particles, their large area would be of great help. For a few years to observe SENS, we could obtain their flux limits as $F \leq 10^{-17} \text{ cm}^{-2} \text{ sec}^{-1} \text{ sr}^{-1}/\epsilon$ with the detection efficiency ϵ . The flux limits are, however, not estimated here since the detection efficiencies are also difficult for us to evaluate.

The TA (telescope array project) with effective aperture of $S\Omega\epsilon = 6 \times 10^3 \text{ km}^2 \text{ sr}$ ($S\Omega = 6 \times 10^4 \text{ km}^2 \text{ sr}$ and the duty factor $\epsilon = 0.1$) is planned to detect cosmic rays with energy $10^{16} - 10^{20}$ eV [27], by detecting the air fluorescence. Using some special trigger, it may detect slow par-

ticles with large energy loss [28]. With such a trigger, it may be able to search for SENS flux at the level of $F < 1 \times 10^{-21} \text{ cm}^{-2} \text{ sec}^{-1} \text{ sr}^{-1}$, if the fluorescence light yield of the event is equivalent to that of air showers of the minimum energy $E_{\min} = 10^{16} \text{ eV}$. Considering energy release of roughly 1 GeV per absorbed nucleon in the KKST process, one obtains the condition of detectability in TA

$$\sigma \int \rho dx \geq E_{\min} / \xi_{\text{SENS}}, \quad (12)$$

where ξ_{SENS} is the ratio of the efficiency of fluorescence light yield per total energy loss of SENS to that of extensive air showers. In the KKST process we estimate $\xi_{\text{SENS}} \sim 1$, since emitted pions are relativistic. Assuming the average density of air $\rho \sim 0.5 \times 10^{-3} \text{ g/cm}^3$ and the path length of SENS in the atmosphere $L \sim 20 \text{ km}$, we obtain the lower limit of SENS mass from Eq. (12)

$$M_Q > 0.7 \times 10^{24} \left(\frac{M_S}{\text{TeV}} \right)^4 \text{ GeV}.$$

The OA (Owl-Airwatch) detector [42] on a satellite with effective aperture $5 \times 10^5 \text{ km}^2 \text{ sr}$ (with duty cycle of 0.2 taken into account) to observe the atmospheric fluorescence of air showers with energy $10^{19} - 10^{20} \text{ eV}$ or more. If it could also detect slow particles with high efficiency, it would be able to search for SENS for a year at the flux level of $F < 10^{-23} \text{ cm}^{-2} \text{ sec}^{-1} \text{ sr}^{-1}$. For SENS to yield the amount of fluorescence light comparable to that of air showers with 10^{19} eV , their mass should satisfy $M_Q > 2 \times 10^{28} (M_S/\text{TeV})^4 \text{ GeV}$.

The bounds given in the various experiments mentioned above are summarized in Fig. 1(a). This figure also gives the flux to be expected if the dark matter of the Galaxy consists mainly of SENS [see Eq. (7)]. Note that these bounds of excluded regions depend on M_S . (The lower mass bound in each experiment is calculated taking $M_S = 1 \text{ TeV}$ in this figure. In case of TA and OA, we added those for $M_S = 100 \text{ GeV}$.) The region, which the future experiments are expected to be able to search, are also given there. If we assume that the dark matter of the Galaxy consists mainly of SENS, i.e., if the flux is just on the DM limit line of Fig. 1(a), we obtain the excluded regions of SENS mass as functions of the parameter M_S as in Fig. 1(b). This figure shows that SENS with the U(1) charge $Q \geq 10^{22}$ are interesting cosmologically in the region of $M_S \geq 6 \times 10^3 \text{ GeV}$, while that TA and OA could search for SENS of $10^{25} \leq Q \leq 10^{35}$ in the region of $M_S \leq 6 \times 10^3 \text{ GeV}$.

C. Bounds on Flux and Mass of Charged Q balls (SECS)

Charged Q balls (SECS) interact with matter in a way similar to nuclearites [18,19]. The rate of energy loss of SECS in matter is

$$\frac{dE}{dx} = -\sigma \rho v^2, \quad (13)$$

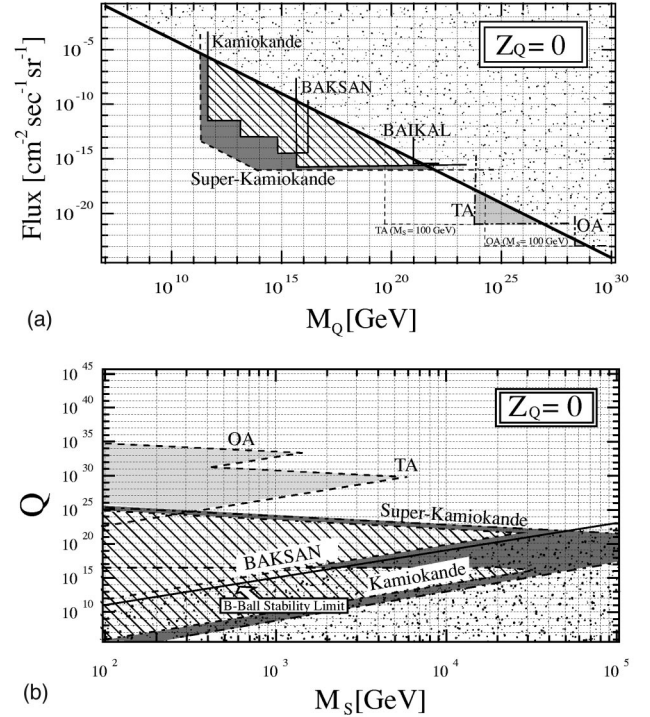


FIG. 1. (a) Bounds on flux and mass for neutral Q balls ($Z_Q = 0$), i.e., SENS. The diagonal line shows the flux expected in case that the Galaxy dark matter ($\sim 0.3 \text{ GeV/cm}^3$) consists mainly of SENS, and thus the region above this DM line with dilute random dots should be excluded. The regions (hatched with solid lines) excluded by the present or past experiments shown here are based on the monopole search experiments with monopole-catalyzed proton decay (the Rubakov effect, see text for details). The regions to be searched by the future or present experiments are shown with half-tone dot meshing. The lower mass bound in each experiment is calculated taking $M_S = 1 \text{ TeV}$ (taking also $M_S = 100 \text{ GeV}$ for TA and OA). The experiments shown here are Kamiokande [22], Gyrlyanda [11], BAKSAN [12], super-Kamiokande, AMANDA [25,26], TA [27,28], and OA [42]. (b) Bounds on the U(1) charge Q versus the symmetry breaking scale M_S for SENS ($Z_Q = 0$) in case of the Galaxy dark matter consisting mainly of SENS [the flux and mass of SENS in this case is restricted to lie on the diagonal line of (a)]. The allowed region $Q \geq 10^{22}$ is only the upper blank part of the figure. The line with the “B-ball stability limit” shows that only the region above it is allowed to have the stability of SENS in case they are B balls (see text for details).

where σ is the cross section of SECS collision with the matter, ρ is the density of the matter, and v is the relative velocity of SECS and the matter. Substituting $E = (1/2)M_Q v^2$ in the above equation and integrating with respect to x , one obtains

$$\rho L = \frac{M_Q}{\sigma} \ln \frac{v_0}{v_c}, \quad (14)$$

where L is the range of SECS in the medium, v_0 is an initial velocity of SECS ($\sim 3 \times 10^7 \text{ cm/sec}$), and v_c is a final velocity of SECS for which we use the estimation in case of nuclearites, $v_c \sim 1.7 \times 10^4 \text{ cm/sec}$ in rock [19]. SECS with

velocity below this value are quickly brought to rest. In case of SECS with radius larger than 1 Å, i.e., $M_Q > 2.1 \times 10^{30} (M_S/\text{TeV})^4$ GeV, the cross section is simply given by $\sigma = \pi R_Q^2$. From Eqs. (4), (5), and (14), we obtain

$$\rho L = 6.2 \times 10^{12} \left(\frac{M_S}{\text{TeV}} \right)^{8/3} \left(\frac{M_Q}{\text{GeV}} \right)^{1/3} \text{ gr/cm}^2. \quad (15)$$

Such heavy SECS, however, should have too small flux to be detected according to Eq. (7), and thus are not interesting to us. We consider only SECS with radius smaller than 1 Å in the following.

If such SECS have significantly large electric charge ($Z_Q \geq \alpha^{-1} \sim 137$ where α is the fine structure constant), the cross section of their collision with matter is controlled not by their intrinsic radius R_Q but by the size of the surrounding electron cloud which is never smaller than ~ 1 Å. We note the situation is similar to the case of nuclearites [19]. We have $\sigma = \pi R_{\text{eff}}^2$ with $R_{\text{eff}} = 1$ Å, which leads to the relation

$$\rho L = 4.0 \times 10^{-8} \left(\frac{M_Q}{\text{GeV}} \right) \text{ gr/cm}^2. \quad (16)$$

Equation (16) shows that SECS with $Z_Q \geq 137$ should be as heavy as

$$M_Q > 2.5 \times 10^7 \left(\frac{\rho L}{\text{gr/cm}^2} \right) \text{ GeV} \quad (17)$$

in order to penetrate the medium with density ρ and length L .

If the charge of SECS is small $Z_Q \ll 137$ (and the intrinsic SECS radius R_Q is also smaller than 1 Å), the effective cross section should be smaller than $\pi(1 \text{ Å})^2$. We then need more delicate treatments to estimate the energy loss rate. It is known that there are two kinds of interaction contributing to the energy loss of SECS at low velocity $\beta \sim 10^{-3}$, i.e., interaction with electrons and interaction with nuclei $dE/dx = (dE/dx)_{\text{electrons}} + (dE/dx)_{\text{nuclei}}$ [14,29–33]. The electronic energy loss rate is estimated as [29]

$$\left(\frac{dE}{dx} \right)_{\text{electrons}} = 8 \pi \alpha a_0 \frac{v}{v_0} N_e \frac{Z_Q^{7/6}}{(Z_Q^{2/3} + Z^{2/3})^{3/2}}, \quad (18)$$

where v_0 is given by αc , N_e is the number density of electrons in the medium, Z is the atomic number of the medium, and a_0 is the Bohr radius. The rate of energy loss caused by interaction with the nuclei of the medium given as [32]

$$\left(\frac{dE}{dx} \right)_{\text{nuclei}} = 4 \pi \alpha a N_Z Z_Q Z \frac{M_Q}{M_Q + M} \frac{A \ln B \epsilon}{B \epsilon - (B \epsilon)^{-C}}, \quad (19)$$

with $A = 0.56258$, $B = 1.1776$, $C = 0.62680$, M is the mass of the target nucleus, N_Z is the number density of target nuclei, and

$$\epsilon = \frac{a M M_Q \beta^2}{2 \alpha Z_Q Z (M_Q + M)}, \quad a = \frac{0.8853 a_0}{(\sqrt{Z_Q} + \sqrt{Z})^{2/3}}. \quad (20)$$

In the case of $M_Q \gg M$ we calculated $(dE/dx)_\rho \equiv (dE/dx)/\rho$ (which depends only loosely on the density of the medium) for SiO_2 and obtained $(dE/dx)_\rho = 0.16, 0.41, 0.71$, and 2.9 GeV/gr/cm² for SECS with typical charge $Z_Q = 1, 2, 3$, and 10 , respectively. We also find the energy loss rate $(dE/dx)_\rho$ does not depend much on matter medium (air, water, and/or rock), and we use the above values for the following estimation of energy loss. The condition for SECS to penetrate the medium with density ρ and length L is roughly given by

$$\frac{1}{2} M_Q \beta^2 > \left(\frac{dE}{dx} \right)_\rho \rho L. \quad (21)$$

Since SECS have large cross section in collision with matter unlike SENS, they should have kinetic energy large enough to reach a detector and to penetrate it. Let us take the following experiments as typical ones which would detect SECS.

MACRO with its three subdetectors are sensitive to SECS [14,23,24] for any values of Z_Q ; in order that SECS can reach the underground detector site from above with $\rho L \sim 3.7 \times 10^5$ gr cm⁻², the lower limit of the SECS mass M_Q is given by Eqs. (17) and (21), as $M_Q > 1.2 \times 10^{11}$, 3.0×10^{11} , 5.3×10^{11} , 2.1×10^{12} , and 9.3×10^{12} GeV for $Z_Q = 1, 2, 3, 10$, and 137 , respectively. The flux limit suggested by the results of no events of monopole search experiments [14] is roughly [34] $F \leq 10^{-16}$ cm⁻² sec⁻¹ sr⁻¹. It is obvious that the inclusion of searches for Q balls from below lowers the flux upper limit by a factor of 2, though the lower limits for the mass to reach the detector increase by a factor of $(\rho L)_{\text{from below}}/(\rho L)_{\text{from above}} = (6.6 \times 10^9)/(3.7 \times 10^5) \sim 1.8 \times 10^4$. This feature for SECS is common to other experiments, OYA, NORIKURA, KITAMI, AKENO, UCSDII, KEK, and MICA.

The OYA experiments [35] with CR-39 plastic track detectors located at the depth of $\rho L = 10^4$ cm⁻² sec⁻¹ sr⁻¹ searched for monopoles and nuclearites for 2.1 y. The flux limit of them correspond to that of SECS, $F < 3.2 \times 10^{-16}$ cm⁻² sec⁻¹ sr⁻¹ [34]. Since the detectors are sensitive to the restricted energy loss larger than ~ 0.14 GeV gr/cm², SECS with charge $Z_Q \geq 2$ can be detectable with them. The condition for SECS to reach the detector is $M_Q > 8.2 \times 10^9$, 1.4×10^{10} , 5.8×10^{10} , and 2.5×10^{11} GeV for $Z_Q = 2, 3, 10$, and 137 , respectively.

The KEK experiments with scintillation counters placed at ground level [37] should be sensitive to SECS for any values of Z_Q , since the detection threshold is $0.01 I_{\text{min}}$ where I_{min} is the minimum energy loss of the ionizing particle with $Z = 1$ [34]. We interpret that their flux upper limit for strange quark matter (nuclearites) holds for the SECS, $F < 3.2 \times 10^{-11}$ cm⁻² sec⁻¹ sr⁻¹. The mass bounds for SECS to reach detectors located at ground level are given by $M_Q > 3.1 \times 10^8$, 8.2×10^8 , 1.4×10^9 , 5.8×10^9 , and 2.5×10^{10} GeV for $Z_Q = 1, 2, 3, 10$, and 137 , respectively.

The KITAMI experiments with CN (cellulose nitrate) nuclear track detectors installed in houses at sea level give the flux limit $F < 5.2 \times 10^{-15} \text{ cm}^{-2} \text{ sec}^{-1} \text{ sr}^{-1}$ [36], which we reinterpret as the SECS flux limit [34]. Since the ionization energy loss of SECS should be larger than $\sim 1.3 \text{ GeV/gr/cm}^2$ for chemically etchable track to be made in CN, we estimate that SECS with $Z_Q \geq 10$ can be detected with the CN detectors. At ground level with $\rho L = 10^3 \text{ gr cm}^{-2}$, SECS heavier than 5.8×10^9 and $2.5 \times 10^{10} \text{ GeV}$ can penetrate the atmosphere to reach the detector from above, for $Z_Q = 10$ and 137, respectively.

The AKENO experiments with helium-gas counters [38] located at ground level should be sensitive to SECS for any values of Z_Q . The detector is composed of layers of proportional counters and concrete shields. The detector is sensitive to tracks with ionization larger than $10I_{\text{min}}$, which should assure the detectability for SECS with any value of Z_Q . The SECS with mass $M_Q > 5.8 \times 10^8, 1.5 \times 10^9, 2.6 \times 10^9, 1.1 \times 10^{10},$ and $4.7 \times 10^{10} \text{ GeV}$ can penetrate the earth and the concrete shields of the detector from above for $Z_Q = 1, 2, 3, 10,$ and 137, respectively. Using the results of no events in detection, we estimate the flux limit $F < 1.8 \times 10^{-14} \text{ cm}^{-2} \text{ sec}^{-1} \text{ sr}^{-1}$ [34].

The UCSDII experiments with He-CH₄ proportional tubes placed at ground level [39] should be sensitive to SECS with any values of Z_Q , since the detection threshold is $0.09I_{\text{min}}$. The flux upper limit for monopoles $F = 1.8 \times 10^{-14} \text{ cm}^{-2} \text{ sec}^{-1} \text{ sr}^{-1}$ should be the same as that for SECS [34]. The mass bounds are the same as in the above case of KEK experiments.

The NORIKURA CR-39 experiments were done at the top of Mt. Norikura to search for monopoles and for strange quark matter [40]. They are sensitive to tracks with ionization larger than 0.35 GeV/gr/cm^2 , which assures that SECS with $Z_Q \geq 3$ would be detectable. Since the detector is installed at the high place, it is more sensitive to lighter SECS in comparison with the ground level detectors (such as KITAMI, AKENO, UCSDII, and KEK). The flux limit is obtained as $F = 2.2 \times 10^{-14} \text{ cm}^{-2} \text{ sec}^{-1} \text{ sr}^{-1}$.

The MICA analysis with ancient mica crystals which were $0.6\text{--}0.9 \times 10^9$ y old was made to search for monopoles [13]. It should be also sensitive to SECS with $Z_Q \geq 10$, since the detection threshold is 2.4 GeV/gr/cm^2 [34]. In order to reach the mica crystals at 3 km deep underground with $\rho L = 7.5 \times 10^5 \text{ gr/cm}^2$ from above, SECS should be heavier than $4.4 \times 10^{12} \text{ GeV}$ and $1.9 \times 10^{13} \text{ GeV}$ for $Z_Q = 10$ and 137, respectively. In the case of the monopole search the capture of an aluminum atom by a monopole was taken into account. The detection efficiency was estimated ~ 0.15 and 0 for monopoles from above and for those from below, respectively, due to this consideration. The flux limit was thus made much looser due to this decrease of efficiency. In case of SECS search, however, SECS need not capture an aluminum and can be heavy enough to penetrate the earth. With these considerations we estimate the flux limit for SECS, which is better than that for monopoles by a factor of 6, to have $F = 2.3 \times 10^{-20} \text{ cm}^{-2} \text{ sec}^{-1} \text{ sr}^{-1}$ for SECS from above and a value twice better than this for SECS from all directions.

The SKYLAB experiments with Lexan track detectors installed in the SKYLAB workshop in space reported that no events had detected for superheavy relativistic nuclei ($Z \geq 110$) [16], which correspond to $Z_Q \geq 10$ in our case of slow particles. The Lexan detector and its container have thickness $\rho L = 2 \text{ gr cm}^{-2}$ in total, or effectively $\rho L \sim 3 \text{ gr cm}^{-2}$, which gives the mass lower bound of SECS $M_Q > 1.7 \times 10^7$ and $7.5 \times 10^7 \text{ GeV}$ for $Z_Q = 10$ and 137, respectively. This experiment gives the flux limit of SECS, $F < 3.8 \times 10^{-12} \text{ cm}^{-2} \text{ sec}^{-1} \text{ sr}^{-1}$ [34].

The AMS experiments could detect SECS in the future, if a special trigger for slow particles is possible [41]. Its magnetic spectrometer on the space station would have a large area to get the flux upper limit, $F \times 10^{-11} \text{ cm}^{-2} \text{ sec}^{-1} \text{ sr}^{-1}$ with one year observation [34]. The detection with thickness of the order of $\rho L \sim 10 \text{ gr cm}^{-2}$ needs mass $M_Q > 3.1 \times 10^6, 8.2 \times 10^6, 1.4 \times 10^7, 5.8 \times 10^7,$ and $2.5 \times 10^8 \text{ GeV}$ for $Z_Q = 1, 2, 3, 10,$ and 137, respectively.

The experimental data and also the future possibilities mentioned above are summarized in Figs. 2–6. Figures 2(a)–6(a) represent bounds on the flux and the mass for SECS. Figures 2(a)–4(a) show that the experiments of the future AMS and the present MACRO are very sensitive to a wide parameter region of mass, charge and flux of SECS. On the other hand, Figs. 5(a) and 6(a) show that the SKYLAB and the MICA experiments give us a stringent exclusion of the lower and upper region of mass respectively. Figures 2(b)–6(b) represent bounds on the U(1) charge Q of SECS versus the symmetry breaking parameter M_S in case that the SECS are mainly contributing to the dark matter of the Galaxy. If we assume the SECS are B balls and impose their stability condition, these figures show that only the SECS with $Q \geq 10^{22-26}$ remain to be considered.

So far, we have fixed the velocity of Q balls to be equal to the Virial velocity ($= 10^{-3}c$). It may be interesting, though, to see the velocity dependence of the bounds [46,47]. Our results, however, do not seriously depend on the velocity. In order to see it, we show the dependence of the bounds on the velocity for the case of SECS Q balls with $Z_Q = 1$ as an example. (We have examined all the cases and have found that the bounds depend on the velocity most strongly in this case.) We varied Q ball velocity in the region $2 \times 10^{-4}c \leq v \leq 5 \times 10^{-3}c$, and showed that the bounds on Q of the Q ball with $v = 2 \times 10^{-4}c (\equiv v_-)$ and $v = 5 \times 10^{-3}c (\equiv v_+)$ in Fig. 2(b).

III. EXPERIMENTAL BOUNDS ON FERMI BALLS

A. Fermi-ball properties

We investigate what region is allowed for the flux of Fermi balls in the present section. The Fermi ball, which is another kind of nontopological soliton, was first proposed by Macpherson and Campbell as a candidate of dark matter [3]. The Fermi balls with large radius are found unstable against deformation, and are expected to fragment into very small Fermi balls [3]. The Fermi ball then interacts with matter very weakly and seems too difficult to be detected. Electrically charged Fermi balls were then proposed by Morris to

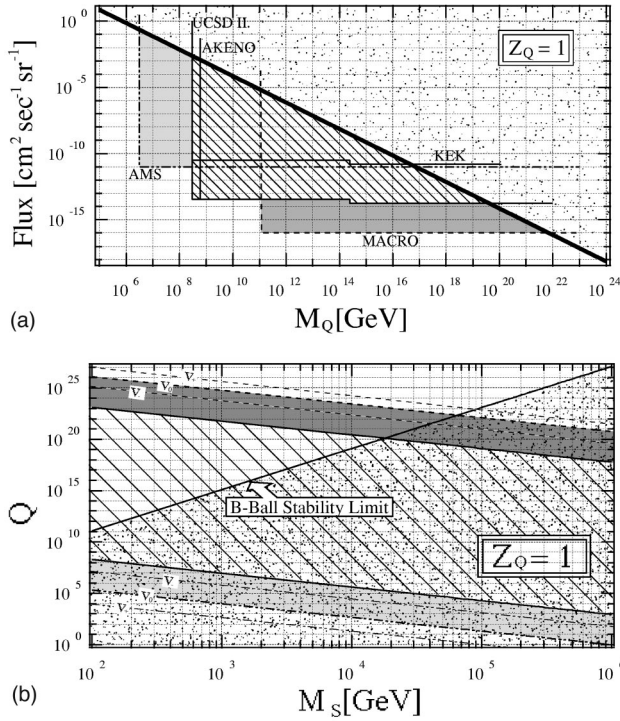


FIG. 2. (a) Bounds on Q ball flux and its mass for SECS with $Z_Q=1$. The diagonal line is the same as in Fig. 1(a) and the region above the line should be excluded. The regions (hatched with solid lines) excluded by the present or past experiments shown here are estimated from the monopole search experiments, nuclearite experiments and other exotic particle searches. The regions to be searched by the future or present experiments are shown with half-tone dot meshing. The experiments shown here are MACRO [14,23,24], KEK [37], AKENO [38], UCSDII [39], and AMS [41]. (b) Represents bounds on Q and M_S of SECS with $Z_Q=1$ (see texts for details.) The marks and patterns to separate regions are the same as those in Fig. 1(b). The boundaries of regions excluded by the possible experiments in case where the Q balls' velocity equals $v_+ \equiv 5 \times 10^{-3}c$ and $v_- \equiv 2 \times 10^{-4}c$, in addition to the case where $v = v_0 \equiv 10^{-3}c$, are also shown in (b) (see texts for details).

improve the stability of the Fermi ball against the deformation and fragmentation [4]. Although a Fermi ball with large fermion number is energetically unstable and could fragment into many smaller Fermi balls, the Coulomb force is expected to suppress the process of fragmentation and to make the lifetime of the large Fermi ball long enough to be practically stable. Owing to the electromagnetic interaction, various detectors get sensitive to Fermi balls. In the present paper we focus on experimental bounds for charged Fermi balls, not on the neutral ones. Let us first briefly review the properties of Fermi balls to make our assumptions and terminologies clear.

The charged Fermi ball consists of three components: a scalar field, a large number of electrically charged heavy fermions, and also a large number of electrons or positrons which partly compensate the electric charge of the heavy fermions. (When we consider the stability of Fermi balls in the following, let us assume that the electric charge of the heavy fermions is positive without loss of generality.) Inside

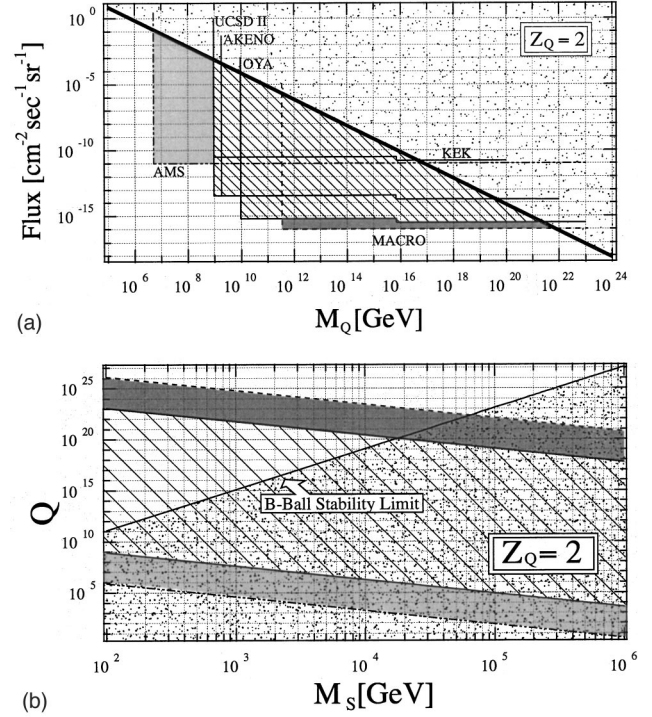


FIG. 3. (a) Bounds on SECS with $Z_Q=2$ similar to Fig. 2(a) apart from the values of mass lower limits and OYA [35] experiments included in (a). (b) Bounds on Q and M_S of SECS with $Z_Q=2$. The marks and patterns to separate regions are the same as those in Fig. 2(b).

the Fermi ball the scalar field has the value of the false vacuum, which is almost degenerate to the true vacuum,⁵ while outside the Fermi ball it has the value of the true one. On the boundary wall, the energy density of the scalar field is higher than those in the two vacua. Since the heavy fermions have a large mass in the true or false vacuum and have a vanishing mass on the wall, many fermions are strongly trapped on it.

Since the electric field of the Fermi ball is strong, electron-positron pairs may be created by quantum field theory effect. This effect decreases the electric field strength by leaving the electrons on the surface and emitting the positrons to infinity. Assuming the difference of the energy density between two vacua to be small enough to be neglected, we obtain the energy of the Fermi ball with the number of heavy fermions N_F and the number of electrons N_e ,

$$E_F = 4\pi\Sigma R^2 + \frac{2(N_F^{3/2} + N_e^{3/2})}{3R} + \frac{\alpha(N_F - N_e)^2}{2R}. \quad (22)$$

Here, Σ is the surface tension of the Fermi ball and R is the radius of it. The radius of the stable Fermi-ball, R_F is deter-

⁵These almost degenerate vacua are necessary for the existence of the large Fermi balls.

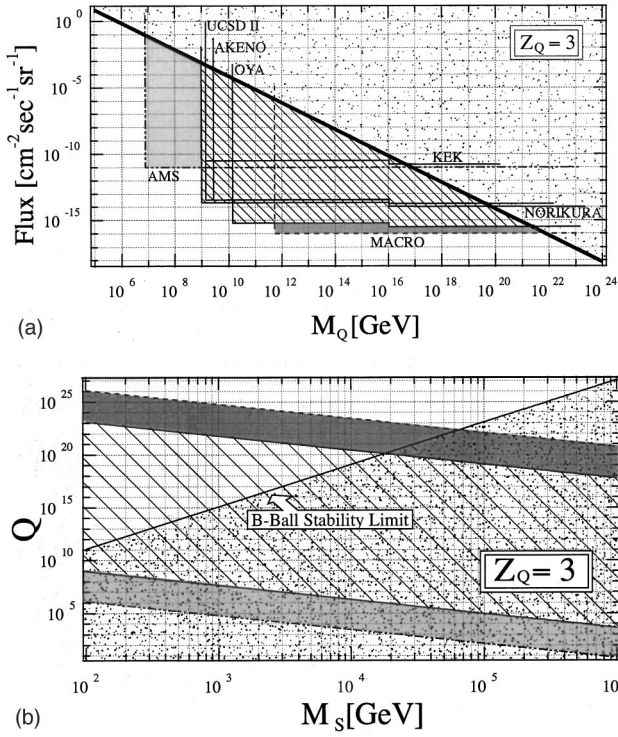


FIG. 4. (a) Bounds on SECS with $Z_Q=3$, similar to Fig. 3(a) apart from the values for excluded mass region and NORIKURA [40] experiments included in (a). (b) Bounds on Q and M_S of SECS with $Z_Q=3$. The marks and patterns to separate regions are the same as those in Fig. 3(b).

mined by balance⁶ of the surface tension energy (the first term) proportional to R^2 , and the Fermi energy (the second term) or Coulomb energy (the third term) which is proportional to R^{-1} as

$$R_F = \left\{ \frac{1}{8\pi\Sigma} \left[\frac{2(N_F^{3/2} + N_e^{3/2})}{3} + \frac{\alpha(N_F - N_e)^2}{2} \right] \right\}^{1/3}. \quad (23)$$

The energy of the Fermi ball is then

$$E_F (= M_F) = 12\pi\Sigma R_F^2 \equiv \kappa^3 R_F^2, \quad (24)$$

which is the common relation when the volume energy can be neglected. Our following analyses of the Fermi-ball's flux are based only on the above relation. The experimental

⁶We have two ways in differentiating Eq. (22) with respect to R : either one fixes N_F and N_e , or one fixes N_F and the electric field \mathcal{E} on the surface of the Fermi ball as the critical value $\mathcal{E} = m_e^2/e$. Here we take the former following Morris [4]. For the other possibility see Ref. [43].

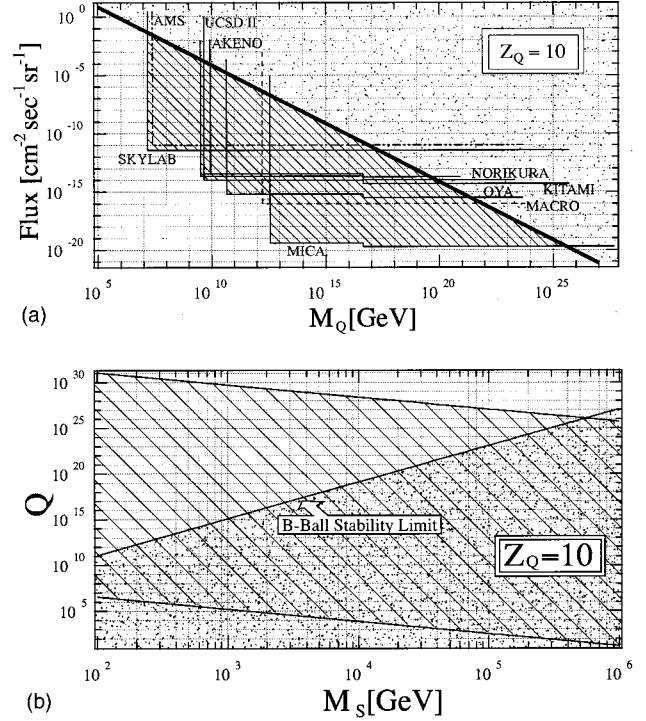


FIG. 5. (a) Bounds on SECS with $Z_Q=10$, similar to Fig. 4(a) apart from the values for excluded mass region and inclusion in (a) of the experiments of SKYLAB [16], KITAMI [36], and MICA [13]. The experiments of MICA and SKYLAB give stringent bounds. (b) Bounds on Q and M_S of SECS with $Z_Q=10$. The marks and patterns to separate regions are the same as those in Fig. 4(b).

bounds from these analyses then do not depend on details of Fermi-ball models.

B. Bounds on flux and mass of Fermi balls

We discuss what physical parameter region is excluded by experiments in the present section. If the electric charge of the heavy fermions is positive, the observational situation is almost the same as the case for SECS with $Z_Q \geq 137$, i.e., the effective radius can be taken as $R_{\text{eff}} \sim 1 \text{ \AA}$ when the intrinsic radius is smaller than this value. In case of the Fermi ball (not as is the case with the Q ball), however, the radius can be larger than 1 \AA without getting too heavy, since its mass is proportional to R_F^2 rather than R_F^3 . The effective radius thus becomes

$$R_{\text{eff}} = \begin{cases} 1 \text{ \AA} & \text{for } R_F < 1 \text{ \AA}, \\ R_F & \text{for } R_F \geq 1 \text{ \AA}. \end{cases} \quad (25)$$

In the case where R_F is large enough, Fermi balls can be detected with not only detectors which are sensitive to SECS with $Z_Q \geq 137$, but also with future detectors for extensive air showers such as TA and OA. This detectability with the future experiments is the main difference from the case of SECS with $Z_Q \geq 137$. We examine the bounds on Fermi

balls⁷ to be given by AMS, SKYLAB, UCSDII, AKENO, KEK, NORIKURA, KITAMI, OYA, MACRO, MICA, TA, and OA in the following.

First we discuss in what conditions the Fermi-ball reaches and penetrates the detectors. For Fermi-balls with $R_{\text{eff}} = 1 \text{ \AA}$ ($R_F < 1 \text{ \AA}$), the condition is the same as that for SECS with $Z_Q \geq 137$, i.e., Eq. (17),

$$M_F > 2.5 \times 10^7 \left(\frac{\rho L}{\text{gr/cm}^2} \right) \text{ GeV}. \quad (26)$$

For Fermi balls with $R_{\text{eff}} = R_F$ ($R_F > 1 \text{ \AA}$), the condition is different from that for SECS [see Eq. (15)], since the relation between the mass and the radius of Fermi balls is different from that of Q balls. Using Eqs. (14) and (24) with $\sigma = \pi R_F^2$, we obtain the condition

$$\kappa \geq 4.7 \times 10^{-2} \left(\frac{\rho L}{\text{gr/cm}^2} \right)^{1/3} \text{ GeV}. \quad (27)$$

This condition is independent of the mass of Fermi balls in case of $R_F \geq 1 \text{ \AA}$. From Eqs. (26) and (27) we see that all the experiments except TA and OA give the same bounds on mass and flux of Fermi balls as on those of SECS with $Z_Q \geq 137$, since the detection efficiencies for these two kinds of solitons are the same for these detectors.

We next discuss the conditions for detecting Fermi balls with TA and OA which need the fluorescence light yield corresponding to the air shower energy of $E_{\text{min}} = 10^{16} \text{ eV}$ for TA [27,28] and $E_{\text{min}} = 10^{19} \text{ eV}$ for OA [42]. This condition is satisfied if the energy loss of the Fermi ball is

$$\pi R_F^2 \rho v^2 L \geq E_{\text{min}} / \xi_F. \quad (28)$$

Here the parameter ξ_F , is the ratio of the efficiency of fluorescence light yield per total energy loss for slow Fermi balls to that for high energy cosmic ray protons. We estimated it from the measurements of the efficiency of ionization for slow ions [31,30] as $\xi_F \sim 1/5$. By taking the average density of air as $\rho = 5.0 \times 10^{-4} \text{ g/cm}^3$, the velocity of the Fermi ball as $v = 10^{-3}c$, and the length of the trajectory as $L = 20 \text{ km}$, one obtains the condition to observe Fermi balls from Eqs. (24) and (28),⁸

$$M_F \geq 6.5 \times 10^{22} \left(\frac{\kappa}{10^3 \text{ GeV}} \right)^3 \left(\frac{E_{\text{min}}}{10^{16} \text{ eV}} \right) \text{ GeV}. \quad (29)$$

⁷In the following we assume that the electric charge of Fermi balls is positive. In the case where Fermi balls have negative electric charge, it is much easier for us to detect them than those with positive charge, since the former may trap nuclei in collision with matter and emit mesons or photons with total energy of order 1 GeV per nucleon. We note all the region excluded for positive Fermi balls should also be excluded for negative Fermi balls.

⁸Here we did not assume the black body radiation from the Fermi-ball trajectory, since it is effective only for dense medium [19].

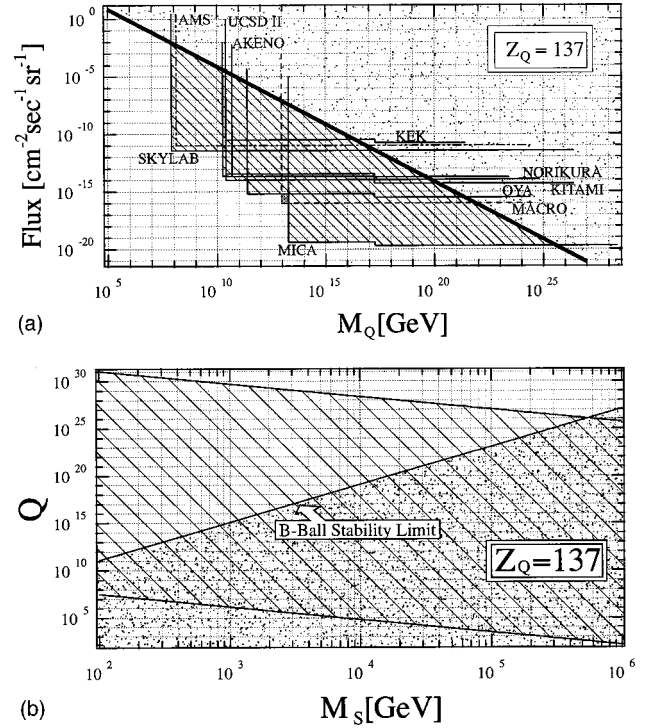


FIG. 6. (a) Bounds on SECS with $Z_Q = 137$, similar to Fig. 5(a) apart from the values for excluded mass region. In this case the cross section for the collision with matter atoms are assumed to be πR_{eff}^2 with $R_{\text{eff}} \sim 1 \text{ \AA}$. We expect that the case with $Z_Q > 137$ is the same as the case with $Z_Q = 137$ (see texts for details). (b) Bounds on Q and M_S of SECS with $Z_Q = 137$. The marks and patterns to separate regions are the same as those in Fig. 5(b).

If TA can observe slow particles,⁹ it will be able to search for Fermi balls to give the same flux limit as that of SENS, $F < 1 \times 10^{-21} \text{ cm}^{-2} \text{ sec}^{-1} \text{ sr}^{-1}$ [27]. Equation (29) gives the mass bounds to observe Fermi balls, $M_F \geq 6.5 \times 10^{22} (\kappa / 10^3 \text{ GeV})^3 \text{ GeV}$. If OA can observe slow particles as well, the flux bounds to be obtained are better by 2 orders of magnitude $F < 1 \times 10^{-23} \text{ cm}^{-2} \text{ sec}^{-1} \text{ sr}^{-1}$ [42], for $M_F \geq 6.5 \times 10^{25} (\kappa / 10^3 \text{ GeV})^3 \text{ GeV}$.

The flux limit with $\kappa = 10^3 \text{ GeV}$ is shown in Fig. 7(a). This figure shows that quite broad regions are already excluded by available experimental data. The future experiments, TA and OA, may have possibility to search large regions which have not been accessible by the existing experiments. Figure 7(b) shows the region of $M_F - \kappa$ plane (hatched with solid lines and with half-tone dot meshing) to be excluded when we assume that the dark matter of the Galaxy consists mainly of Fermi balls.

We here discuss how these results constrain the Morris's simple Fermi-ball model [4]. The electric field becomes the critical value $\mathcal{E} = m_e^2/e$ near the surface due to the surrounding electrons in this model. The third term of Eq. (22) is $m_e^4 R^3 / 2\alpha$ in this case. When this Coulomb energy is related

⁹The TA experiments may be available for a slow particles search with a special trigger [28].

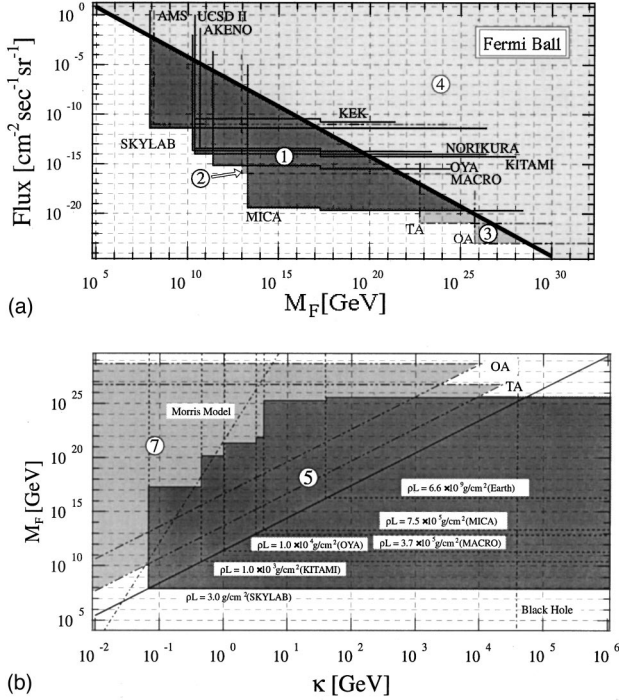


FIG. 7. (a) Bounds on flux and mass of Fermi balls obtained from various experiments. This is similar to Fig. 6(a) (SECS with $Z_Q=137$), though it has additional restrictions to be expected by the future TA and OA experiments. (b) Excluded region in the $M_F-\kappa$ plane. The stair-shaped area hatched by solid lines is excluded by the available data. The region with half-tone mesh would be investigated by the future experiments, TA and OA. The Morris model line [Eq. (30)] and black hole limit [Eq. (31)] are also shown in this figure (taking $C=1$).

to the surface energy as $4\pi\Sigma R^2 = Cm_e^4 R^3/2\alpha$ we obtain¹⁰

$$M_F \sim 3(4\pi\Sigma)^3 \left(\frac{2\alpha}{Cm_e^4} \right)^2 = 6.0 \times 10^{21} C^{-2} \left(\frac{\kappa}{\text{GeV}} \right)^9 \text{ GeV}. \quad (30)$$

To prevent the Fermi ball from forming a black hole, its radius should be larger than the Schwarzschild radius $R_F \geq M_F/M_{\text{pl}}^2$, where M_{pl} is the Planck mass. From this condition, we obtain the following constraint of κ using Eq. (30):

$$\kappa \leq 3.3 \times 10^4 C^{1/6} \text{ GeV}. \quad (31)$$

We draw lines which represent Eqs. (30) and (31) in Fig. 7(b). We find that TA and OA are powerful experiments to search the new region of about $10^{17} \text{ GeV} \leq M_F \leq 10^{29} \text{ GeV}$ in the Morris model (taking $C=1$).

¹⁰Since the surface energy must be the same order as the total energy, C must not be much smaller than unity. Investigation into what range of C is allowed to stabilize the Fermi ball is underway [43].

IV. CONCLUSION

Quantum field theory allows the existence of such nontopological solitons as Q balls and Fermi balls, the stability of which is supported by conservation of a global $U(1)$ charge. These solitons may play important roles in cosmology to solve the problems of the dark matter, the baryogenesis, and the γ ray bursts. In the present paper, we considered Q balls and Fermi balls, which are typical nontopological solitons. We examined what parameter regions, masses, fluxes, charges, and energy scales of Q balls and Fermi balls, are to be excluded by analyzing various existing or future searches for monopoles, nuclearites, and cosmic rays as well as existing results or analyses of the Q ball searches with Gyrlyanda and MACRO. The experiments considered here include (1) underground searches with Gyrlyanda, BAKSAN, Kamio-kande, super-Kamiokande, MACRO, OYA, MICA, and AMANDA, (2) searches on the earth's surface with NORIKURA, KITAMI, KEK, AKENO, UCSDII, and TA, (3) space experiments with SKYLAB, AMS, and OA. We summarized these experimental data and obtained bounds on the mass and the flux of Q balls and Fermi balls. Of course the precise estimation of bounds should be more carefully made by those who did or will do the experiments by themselves. We believe, however, that our rough estimation will give useful information for research of Q balls and Fermi balls.

We first investigated Q balls with electric charge $Z_Q=0$ (SENS), which can be detected through a proton-decay-like process proposed in Ref. [10]. We found that a considerably large region, e.g., $Q \geq 10^{25}$ has already been excluded in $Q-M_S$ plane for $M_S < 100 \text{ GeV}$ only by existing experiments [see Fig. 1(b)], and that a wider region $Q \geq 10^{35}$ could be searched by the future experiments TA and OA. We also found that the region $Q=B \leq 10^{22}$ has been excluded for B balls for any value of M_S .

We next investigated Q balls with $Z_Q=1, 2, 3, 10,$ and 137 (SECS), which interact with matter mainly by electromagnetic force just as nuclearites though the relations between the radius and the mass are quite different. We saw that larger Z_Q gives more stringent bounds on flux and mass of SECS. We found that for the value of $M_S \sim 10^2 \text{ GeV}$, experimental data give more stringent bounds on SECS global $U(1)$ charge than the stability condition of B balls and that Q balls with $Q \geq 10^{22-26}$ still remain to be examined (see Figs. 2–6).

We finally investigated Fermi balls with electric charge $Z_F \geq 137$, which are expected to be rather stable against perturbative deformation and fragmentation. We obtained bounds on mass of Fermi balls, $M_F \leq 10^8 \text{ GeV}$ and $M_F \geq 10^{29} \text{ GeV}$ for $\kappa \geq 0.1 \text{ GeV}$ in $M_F-\kappa$ plane. If we further assume Morris Model [4], we obtained more stringent constraints. We noted the importance of the future TA and the OA experiments also for the Fermi balls as seen in Fig. 7(b).

We lastly note that the relatively light charged solitons with $M \leq 10^8 \text{ GeV}$, which we have not discussed much, have astrophysical difficulties, namely, the Galaxy-halo infall, too much heating of disk molecules, and too small density fluctuations in the early universe, if we consider that the

dark matter consists mainly of such solitons with large cross section with matter and radiation. We are thus interested in the window for the heavier charged solitons [44,45].

From these experimental bounds, we comprehensively obtained the stringent bounds on the properties of Q balls and the Fermi balls and then noted the possible importance of the future experiments TA and OA. These bounds will help us study the unsolved cosmological problems above

mentioned by making more realistic scenarios, in which Q balls and/or Fermi balls play an essential role.

ACKNOWLEDGMENTS

We thank H. Tawara, M. Fukugita, M. Fukushima, M. Sasaki, and A. Kusenko for useful comments.

-
- [1] S. Coleman, Nucl. Phys. **B262**, 263 (1985).
 [2] A. Kusenko and M. Shaposhnikov, Phys. Lett. B **418**, 46 (1998).
 [3] A. L. Macpherson and M. A. Campbell, Phys. Lett. B **347**, 205 (1995).
 [4] J. R. Morris, Phys. Rev. D **59**, 023513 (1999).
 [5] B. Holdom, Phys. Rev. D **36**, 1000 (1987); B. Holdom and R. A. Malaney, Astrophys. J. Lett. **420**, L53 (1994).
 [6] K. Enqvist and J. MacDonald, Phys. Lett. B **425**, 309 (1998).
 [7] R. Brandenberger, I. Halperin, and A. Zhitnitsky, hep-ph/9903318.
 [8] S. Kasuya and M. Kawasaki, Phys. Rev. D **61**, 041301 (2000); **62**, 023512 (2000).
 [9] A. Kusenko, M. Shaposhnikov, P. G. Tinyakov, and I. I. Tkachev, Phys. Lett. B **423**, 104 (1998).
 [10] A. Kusenko, V. Kuzmin, M. Shaposhnikov, and P. G. Tinyakov, Phys. Rev. Lett. **80**, 3185 (1998).
 [11] I. A. Belolaptikov *et al.*, astro-ph/9802223.
 [12] E. N. Alexeyev *et al.*, Lett. Nuovo Cimento Soc. Ital. Fis. **35**, 413 (1982).
 [13] P. B. Price and M. H. Salamon, Phys. Rev. Lett. **56**, 1226 (1986).
 [14] D. Bakari *et al.*, hep-ex/0003003.
 [15] Donald E. Groom, Phys. Rep. **140**, 323 (1986); V. V. Iarovski *et al.*, hep-ph/9909528; Particle Data Group, C. Caso *et al.*, Eur. Phys. J. C **3**, 1 (1998), p. 741, and references therein.
 [16] E. K. Shirk and P. B. Price, Astrophys. J. **220**, 719 (1978).
 [17] A. Kusenko, Phys. Lett. B **406**, 26 (1997).
 [18] E. Witten, Phys. Rev. D **30**, 272 (1984).
 [19] A. De Rújula and S. L. Glashow, Nature (London) **312**, 734 (1984).
 [20] V. A. Rubakov, Pis'ma Zh. Éksp. Teor. Fiz. **33**, 658 (1981) [JETP Lett. **33**, 644 (1981)]; C. G. Callan, Jr., Phys. Rev. D **26**, 2058 (1982).
 [21] J. Arafune and M. Fukugita, Phys. Rev. Lett. **50**, 1901 (1983).
 [22] T. Kajita *et al.*, J. Phys. Soc. Jpn. **54**, 4065 (1985).
 [23] Fabrizio Cei for the MACRO Collaboration, hep-ex/9810012.
 [24] M. Ambrosio *et al.*, Eur. Phys. J. C **13**, 453 (2000).
 [25] S. Barwick *et al.*, Contribution to "Proceedings of Astrophysical Aspects of the Most Energetic Cosmic Rays," Japan, 1990.
 [26] AMANDA Collaboration, Proceedings of ICRC 99, Salt Lake City, 1999, edited by D. Kieda *et al.*, Vol 2, p. 344, and references therein.
 [27] M. Fukushima, a talk at the 4th International RESCEU Symposium, "The Birth and Evolution of the Universe," 1999, Tokyo; Y. Arai *et al.*, Proceedings of the 26th International Cosmic Ray Conference, Salt Lake City, 1999, Vol. 5, p. 393.
 [28] M. Sasaki (private communication).
 [29] J. Lindhard and M. Scharff, Phys. Rev. **124**, 128 (1961), and references therein.
 [30] J. A. Phipps *et al.*, Phys. Rev. **135**, A36 (1964).
 [31] Gilbert L. Cano, Phys. Rev. **169**, 277 (1968).
 [32] W. D. Wilson, L. G. Haggmark, and J. P. Biersack, Phys. Rev. B **15**, 2458 (1977).
 [33] D. J. Ficenec *et al.*, Phys. Rev. D **36**, 311 (1987).
 [34] Needless to say, the precise estimation of flux limits or mass bounds of such experiments should be given by the experiment group by themselves with careful examination of the efficiencies of their detectors. We give here only the order of magnitudes though we think even such rough estimations may help some of those who are interested in Q ball flux. In case of the experiments of OYA [35] and NORIKURA [40], one of the present authors, S.N., is a member of the experiment group, who is rather familiar with these experiments.
 [35] S. Orito *et al.*, Phys. Rev. Lett. **66**, 1951 (1991).
 [36] T. Doke *et al.*, Phys. Lett. **129B**, 370 (1983).
 [37] K. Nakamura *et al.*, Phys. Lett. **161B**, 417 (1985).
 [38] T. Hara *et al.*, Phys. Rev. Lett. **56**, 553 (1986).
 [39] K. N. Buckland *et al.*, Phys. Rev. D **41**, 2726 (1990).
 [40] S. Nakamura *et al.*, Phys. Lett. B **263**, 529 (1991).
 [41] J. Alcaraz *et al.*, Phys. Lett. B **461**, 387 (1999); J. Derkaoui *et al.*, Astropart. Phys. **9**, 173 (1998).
 [42] L. Scari, Proceedings of 26th International Cosmic Ray Conference, 1999, Salt Lake City, edited by D. Kieda *et al.*, Vol. 2, p. 384.
 [43] J. Arafune, K. Ogure, and T. Yoshida (in preparation).
 [44] G. D. Starkman, A. Gould, R. Esmailzadeh, and S. Dimopoulos, Phys. Rev. D **41**, 3594 (1990).
 [45] G. D. Starkman, A. Gould, R. Esmailzadeh, and S. Dimopoulos, Nucl. Phys. **B333**, 173 (1990).
 [46] M. Axenides *et al.*, Phys. Rev. D **61**, 085006 (2000).
 [47] R. Battye and P. Sutcliffe, hep-th/0003252.